Bursts of beta oscillation differentiate postperformance activity in the striatum and motor cortex of monkeys performing movement tasks

Joseph Feingold[1], Daniel J. Gibson[1], Brian DePasquale, and Ann M. Graybiel[2]

McGovern Institute for Brain Research and Department of Brain and Cognitive Sciences, Massachusetts Institute of Technology, Cambridge, MA 02139

Contributed by Ann M. Graybiel, September 4, 2015 (sent for review July 3, 2015; reviewed by Helen Bronte-Stewart and Andrew Sharott)

Studies of neural oscillations in the beta band (13–30 Hz) have demonstrated modulations in beta-band power associated with sensory and motor events on time scales of 1 s or more, and have shown that these are exaggerated in Parkinson's disease. However, even early reports of beta activity noted extremely fleeting episodes of beta-band oscillation lasting <150 ms. Because the interpretation of possible functions for beta-band oscillations depends strongly on the time scale over which they occur, and because of these oscillations' potential importance in Parkinson's disease and related disorders, we analyzed in detail the distributions of duration and power for beta-band activity in a large dataset recorded in the striatum and motor-premotor cortex of macaque monkeys performing reaching tasks. Both regions exhibited typical beta-band suppression during movement and postmovement rebounds of up to 3 s as viewed in data averaged across trials, but single-trial analysis showed that most beta oscillations occurred in brief bursts, commonly 90–115 ms long. In the motor cortex, the burst probabilities peaked following the last movement, but in the striatum, the burst probabilities peaked at task end, after reward, and continued through the postperformance period. Thus, what appear to be extended periods of postperformance beta-band synchronization reflect primarily the modulated densities of short bursts of synchrony occurring in region-specific and task-time-specific patterns. We suggest that these short-time-scale events likely underlie the functions of most beta-band activity, so that prolongation of these beta episodes, as observed in Parkinson's disease, could produce deleterious network-level signaling.

basal ganglia | local field potentials | beta band | sequential movement | synchronization

Oscillations of brain activity in the beta band (13–30 Hz) have been implicated in sensorimotor control and integration (1–5) and are pathologically synchronized and exaggerated in Parkinson's disease (6–11). Although reports have published examples of very brief (<150 ms) bursts of beta-band oscillation (12–15), the analysis of beta-band activity has focused primarily on data averaged over trials, which show variations in average beta-band power occurring on a time scale of seconds.

To address the apparent discrepancy in time scales between the single-trial results and the trial-averaged results, we analyzed the relationship of brief beta bursts as viewed at a single-trial level to the substantially slower variations in trial-averaged power that are conventionally referred to as periods of "synchronization" or "desynchronization" of beta-band activity. We examined beta-band activity recorded in two regions of prime clinical interest, the motor-premotor regions of the neocortex and the striatum, in macaque monkeys performing well-learned movement sequences. Our findings suggest that these regions exhibit different peak times of synchronization of beta bursting during the classic postmovement period, comprising differentially timed alignments of beta bursts within a desynchronized background of beta activity. Such brief, one to several cycle alignments of beta oscillation are suitable for realignment of circuit activity according to contextual demands. We suggest that the prolongation of beta bursts known to occur in Parkinson's disease could blunt or abolish such flexibility in the neural control of behavior.

Results

We recorded local field potentials (LFPs) from multiple microelectrodes placed in the primary motor and premotor cortex and the caudate nucleus (CN) and putamen of two female monkeys (Fig. 1*B* and Fig. S1). Visual cues instructed the monkey to perform either a single joystick movement to a peripheral target and back to the center position (1M1T; Fig. 1*A*), or a series of three such movements (3M3T; Fig. 1*C*). Each movement had to be preceded by holding the joystick in the center for a short (0.6–1.2 s) or long (1.4–2.0 s) period that the monkey had to estimate by itself.

As viewed in grand average spectral power over all electrodes in both monkeys (Fig. 1 *D* and *E*), beta power was clearly task-modulated. In each region, beta power fell sharply when the empty cues were presented to signal that a trial could be initiated, and it remained low in both regions throughout the execution of the task. Beta power reached its highest level in the motor-premotor cortex abruptly after cessation of the last movement. In the striatum, beta power also rose postmovement, but peak power was not reached until later in the intertrial interval (ITI), after reward delivery. Similar results were obtained using the method of local average referencing (14) in two sessions (Fig. S2), indicating that volume conduction contributed little to the results. Differences between subregions of the striatum were less marked than the

Significance

Studies of beta oscillations, highlighted clinically because of exaggerated beta-band activity in Parkinson's disease, have focused on measures averaged over multiple trials, and readers outside the field could have the misperception that beta oscillations persist over seconds. We show that brief bursts of oscillation are responsible for virtually all beta-band activity in healthy monkeys. The state called "beta synchronization" consists of numerous brief (~40–120 ms) bouts of oscillation within a nonoscillatory background, and these bouts can also occur during periods of "desynchronization." Thus, postmovement "synchronization" of beta represents a transient increase in oscillation probability, with different time courses in the motor cortex and striatum. We suggest that the timing and duration of these bursts are critical parameters for network function.

Author contributions: J.F. and A.M.G. designed research; J.F. and B.D. performed research; D.J.G. analyzed data with input from J.F. and A.M.G.; D.J.G. and A.M.G. wrote the paper; and A.M.G. oversaw the project.

Reviewers: H.B.-S., Stanford University; and A.S., University of Oxford.

The authors declare no conflict of interest.

[1]J.F. and D.J.G. contributed equally to this work.

[2]To whom correspondence should be addressed. Email: graybiel@mit.edu.

This article contains supporting information online at www.pnas.org/lookup/suppl/doi:10.1073/pnas.1517629112/-/DCSupplemental.

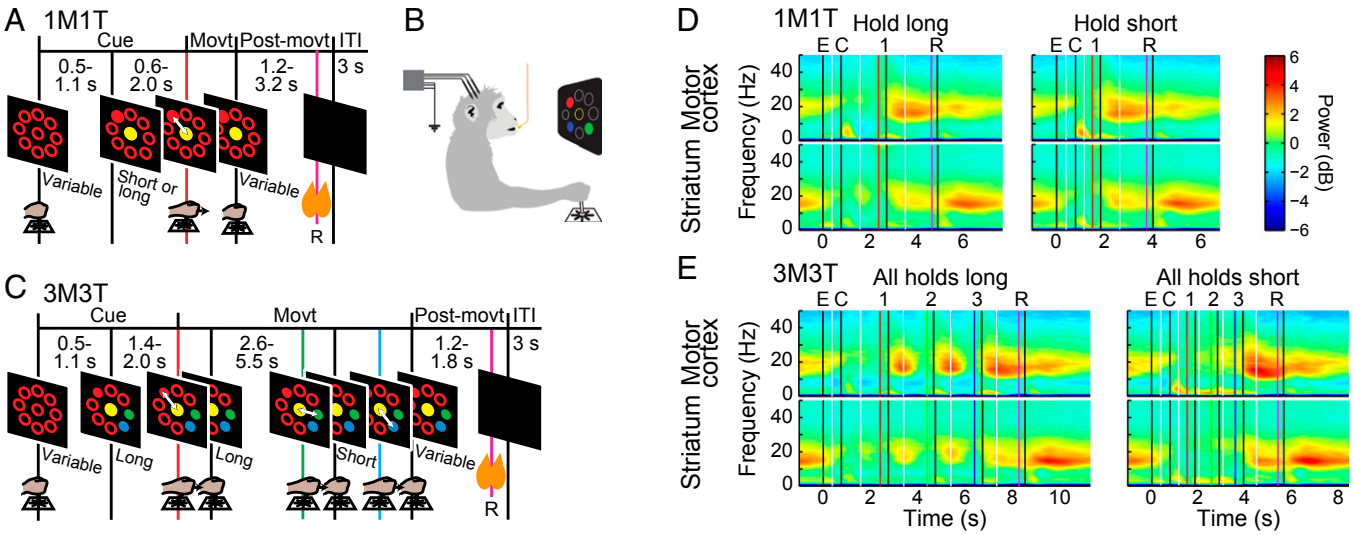

Fig. 1. Overview of tasks and power spectra. (*A* and *C*) Task timelines. (*B*) Monkey's position during the task. (*D* and *E*) Average LFP spectrograms calculated over all correct trials of 1M1T (*D*) and 3M3T (*E*) tasks across two monkeys for each region, using a 1-s moving window. Power is shown in decibels relative to a $1/f^{1.5}$ curve fitted to each channel. White vertical lines mark the boundaries between panels aligned to different task events. Colored vertical lines mark task events: empty targets on (E, black); colored cue targets on (C, black); first movement (1, red); second movement (2, green); third movement (3, blue); reward delivery (R, purple); ends of movements or reward delivery (unlabeled, black).

difference between the striatum and the motor cortex, although local-average-referenced analyses indicated that the moderate increase in striatal beta power at movement cessation is due largely to activity in the putamen, where beta power after movement cessation may be nearly equal to that during the ITI (Figs. S3 and S4). An analysis of coherence in two sessions (Fig. S5) indicated that the regions recorded from were functionally connected in the beta band during the ITI. In one session (HH092807), coherence was stronger immediately after movement cessation, possibly owing to the fact that the motor-premotor cortical electrodes were located more posteriorly in this implant.

Changes in Beta-Band Power in Single Trials Occur Much Faster Than Those Detectable in Averages over Trials. There was a striking contrast between the time courses of beta power fluctuations visible in trial-averaged and single-trial analyses (Fig. 2). Whether averaged with a 1-s analysis window that produced strong temporal smoothing (Fig. 2 *A* and *D*) or plotted with minimal smoothing (Fig. 2 *B* and *E*), the time courses of increased beta span seconds. In the single trial traces (Fig. 2 *C* and *F*), instead of such long periods of increased beta power, there were many short-duration episodes of increased power that become denser during the periods that appeared as synchronized beta activity in the trial-averaged plots. The lack of consistency from trial to trial cannot be accounted for by variations in task demands, because all of the trials shown had the same spatial and temporal patterns of visuomotor requirements. Such inconsistency was typical of the entire dataset, indicating that the trial-averaged analyses blurred brief, often nonsynchronous episodes of beta-band activity. Thus, synchronized beta activity actually comprised many bursts, only some of which were synchronized over successive trials.

Beta-Band Power Is More Variable in LFPs Than in Random Surrogate Data. As a control to determine whether the trial-to-trial variability was different from that produced by random signals, we constructed randomized surrogate signals that were spectrally matched to each channel of actual data for 3M3T blocks (*SI Materials and Methods*). The resulting signals had a temporal structure equivalent to random noise (compare Fig. 2 and Fig. S6). We then calculated the coefficient of variation (CV) of beta power across the entire 3M3T block for both the original signals and the randomized signals (Fig. 3). The CVs for randomized signals fell almost entirely into just one bin; those for the actual data were all higher than any value obtained from any randomized channel, and covered a range of values (Table 1). A paired-sample *t* test showed the difference to be significant ($P < 5 \times 10^{-69}$).

Beta Bursts Come in All Shapes and Sizes. We marked bursts in each channel whenever power in the beta band met or exceeded a threshold of 3 times the median power for that channel (Fig. 4). All surrounding samples for which power was at least 1.5 times the median were considered part of the burst. We recorded the duration, maximum power, and mean power of each identified burst. Because maximum power and mean power were highly correlated (Pearson's rho = 0.93), we pursued analyses of mean power and duration only. As shown in Fig. 5, although peaks of the distributions of duration and power were located in the same bin for the randomized and actual data (90–113 ms duration, 2.4–2.55 times the median power; see also "Burst Marking and Burst Parameter Distributions" in *SI Materials and Methods*), the tails of the distributions were radically different. The burst parameters clustered much more tightly around the peak in the randomized data than in the actual data. We verified that it was reasonable to aggregate bursts across monkeys, regions, tasks, and task periods by plotting each combination separately (Fig. 5*C* and Fig. S7). The contour lines indicate that the apparent difference in tail size was due mainly to the different sizes of the datasets.

The Proportions of High Values of Burst Power and Duration Depend on Task Time. During the cue period, the distributions of burst parameters in real and randomized data appeared similar (Fig. 6 *A* and *C* and Figs. S8 and S9), but extremely high values were more common in the real data (Fig. 6 *B* and *D*). Such extreme values were particularly common during the postmovement and ITI periods (Fig. 6 *E*–*L*), so that the peaks of the real distributions fell below the peaks of the randomized distributions. Strikingly, the extreme values for motor cortex and striatum effectively traded places between the postmovement period and the ITI (Fig. S8); the largest tails in the motor cortex occurred postmovement, whereas in the striatum they were maximum during the ITI.

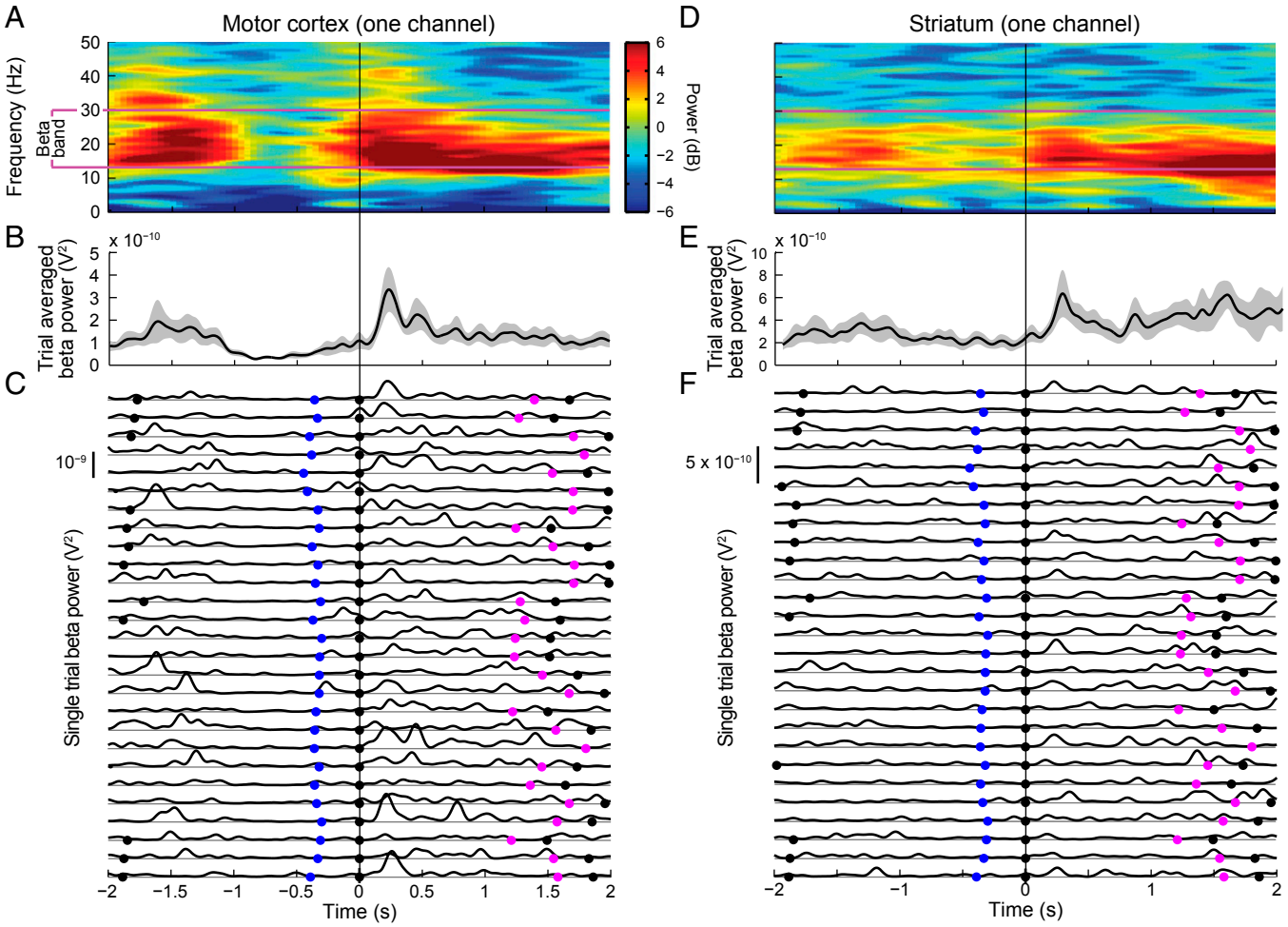

Fig. 2. Examples of LFP activity recorded on individual channels from motor cortex (*A*–*C*) and striatum (*D*–*F*) in one session from 2 s before until 2 s after the end of the third (final) movement. (*A* and *D*) Spectrograms averaged over 27 correct 3M3T trials with the long-long-long hold sequence and the up/left-down-left spatial sequence, with power coded as in Fig. 1. Purple lines denote the beta band. The color scale in *A* applies to *D* as well. (*B* and *E*) Time course of average power in the 13–30 Hz pass band (black lines) with 95% confidence limits (gray shading). (*C* and *F*) Smoothed power traces for each of the 27 trials. The gray horizontal lines below each trace represent zero power. Blue, purple, and black dots mark the onset of third movement, reward delivery, and end of movements/reward delivery, respectively.

Modulations of Trial-Averaged Beta Power Primarily Reflect Modulations of Burst Density. The motor cortex and the striatum exhibited the same reversal between postmovement and ITI in burst density that they showed for burst power and burst duration (Fig. 7); cortical burst density was higher during postmovement, and striatal burst density was higher during ITI. Most of the variations in power were expressed by variations in burst density. The one notable exception was the sharp peak in motor cortex power after termination of the final movement, which was absent or much reduced in the burst density traces. To account for this feature of the trial-averaged power, a change in other burst parameters must be invoked, for example, a brief increase in burst power or a decrease in variability of timing of the first burst after movement termination.

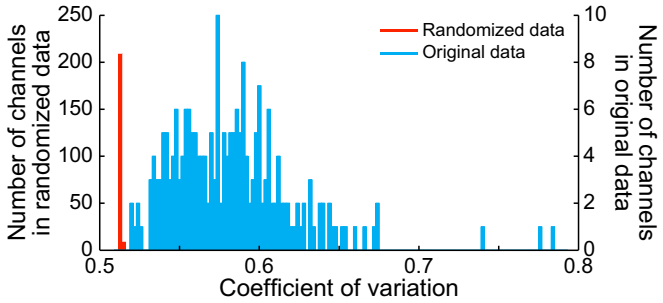

Fig. 3. Distributions of the CV of beta-band power across all channels in all sessions of both monkeys (blue), and across their phase-randomized counterparts (red). Owing to the extreme disparity in the shapes of the two distributions, a different vertical scale is used for each one.

Discussion

Our findings demonstrate that beta-band events in LFPs occur predominantly in brief bursts both in the motor-premotor cortex and in the striatum of monkeys performing self-timed movement tasks, and show that the probability of bursting in both regions is

Table 1. CV for each channel and its matching randomized signal (n = 197)

Data type	Minimum	Maximum	Mean	SD
Actual data	0.520	0.785	0.583	0.0395
Randomized data	0.512	0.513	0.512	0.000297

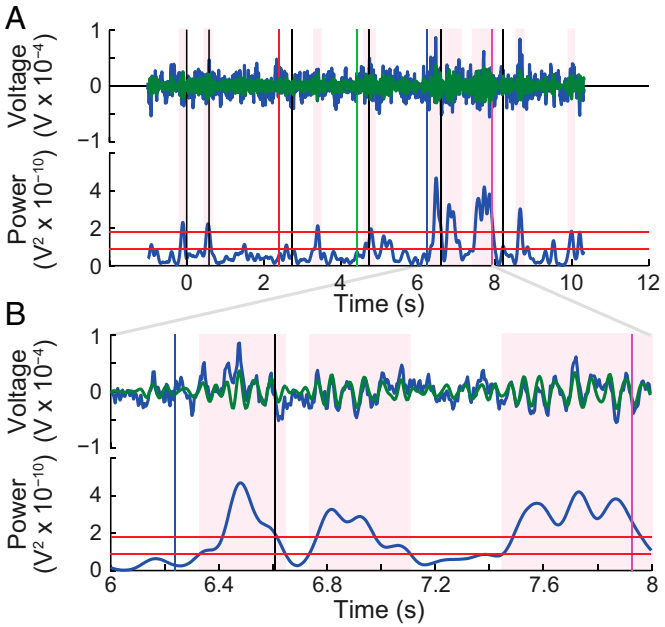

Fig. 4. Procedure for measuring beta bursts illustrated for LFP recorded in the motor cortex in a single trial. Events are shown as in Fig. 1. (*A*, *Upper*) Raw LFP (blue) and beta bandpass-filtered LFP (green) superimposed. (*Lower*) Beta-band power together with red horizontal lines at the two thresholds used (1.5 times and 3 times the median power, respectively). Shading indicates individual burst periods. (*B*) Same data as in *A* on an expanded time scale.

heightened after completion of the ongoing task. The brevity of many of the beta bursts is striking, comprising only one to several cycles of beta. Even during task periods in which beta bursts were most likely to occur, the chance of seeing a burst never exceeded 55% (Fig. 7 and Table S1). Thus, beta synchronization and desynchronization are quantum-mechanics-like probabilistic states, reflecting the probability of much shorter bursts of oscillation rather than the strength of sustained oscillations. The task-selective modulation of these probabilistic states suggests a functional import for the oscillations that must be realized during their short lifetimes.

Notably, we found that the timing of the episodes of posttask beta bursting were largely different in the two regions. In the motor-premotor cortex, peak beta-burst probabilities occurred in the immediate postmovement period, corresponding to the time classically referred to as postmovement resynchronization. In the striatum, although there were some sites, especially in the putamen, at which beta bursts were prominent in the postmovement period, for the most part the maximum beta bursting occurred later, during the ITI that followed reward and task end. Thus, postperformance beta oscillations in the motor cortical region appear to be related to movement completion, as indicated in classic studies, but striatal beta oscillations on average mark task end twice as strongly as movement completion. This late striatal postperformance beta-band activity accords with the occurrence of brief spike activity peaks recorded in the striatum and prefrontal cortex of both monkeys and rodents after task completion (16–20).

Our work emphasizes the fast dynamics of beta activity. Early studies in humans and nonhuman primates prominently featured such brief bursts of beta oscillations (12–14), but the majority of later studies have concentrated on trial-averaged views of beta modulation, obscuring the very fast dynamics visible in individual trials. The terms "event-related synchronization," "movement-related desynchronization," and "resynchronization" tend to foster the misapprehension that beta oscillations are persistently present or suppressed, when in fact beta power in between bursts in any given trial is low during much of the synchronization, and beta power during bursts can still be relatively high during desynchronization. A recent study that recognized the importance of a fast time scale is that of Cagnan et al. (21), who examined the correlation between beta amplitude and the angle of beta-band phase-locking between the human subthalamic nucleus and globus pallidus during phase-locking events as brief as 50 ms. Similarly brief bursts of gamma oscillation have been found in rodent studies of phase-amplitude coupling (22–24) and movement initiation (25).

Here we focused on the postperformance period, following up on studies of the rodent basal ganglia in which accentuated postperformance beta bursting was documented (15, 26). Numerous studies in nonhuman primates have demonstrated significant task-related effects in the low beta band (4, 5, 27–29), but except for the elegant studies of Tan and colleagues (30, 31), oscillation during the postmovement period has not been analyzed in detail. Brief episodes of heightened spike activity at task end have been documented in both nonhuman primates and rodents (16–20, 32). It has been suggested that the end-signaling could be part of a mechanism to tag completion of successful sequences of behavior, providing action boundaries to facilitate the expression of such action sequences (16, 17). In the ventromedial striatum, such task-end spike and beta-burst activities were found to develop with behavioral learning (26), further suggesting that the LFP beta-burst activity could reflect local neuronal activity patterns and plasticity.

Maintenance of the status quo (33), error evaluation and motor adaptation (30, 31), and task difficulty (12, 13) are among the interpretations given to bouts of heightened beta-band activity in normal subjects. Here we suggest that beta bursts could have different functions in different regions of the brain. For the motor cortex and striatum of monkeys, the critical context that defined the end of the task differed in a way that seemed to match the functional specializations of the two regions: the motor cortical areas for the execution of the movements, and the striatum for modulation of task performance based on cost-benefit analysis through reinforcement-based learning. By extension, in

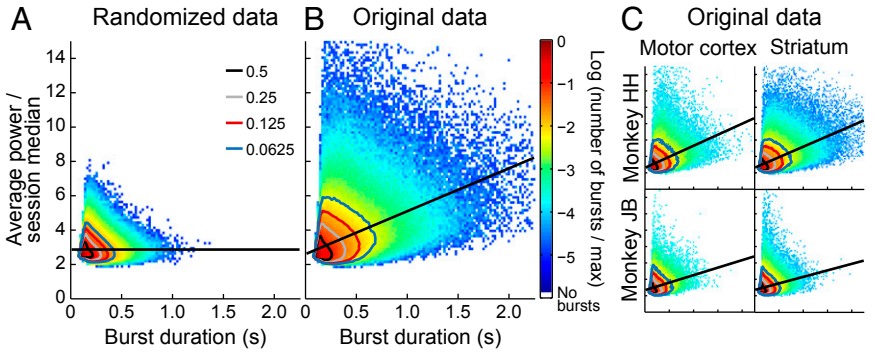

Fig. 5. Joint distribution of duration and power values across all marked beta bursts in the dataset. Contour lines show the boundaries of the tails containing one-half (black), one-quarter (gray), one-eighth (red), and one-sixteenth (blue) of the counts. Straight black lines show least squares fits. (*A*) Phase-randomized control channels. (*B*) Actual (non-randomized) LFPs. (*C*) Same data as in *B*, but plotted separately for monkey and brain region.

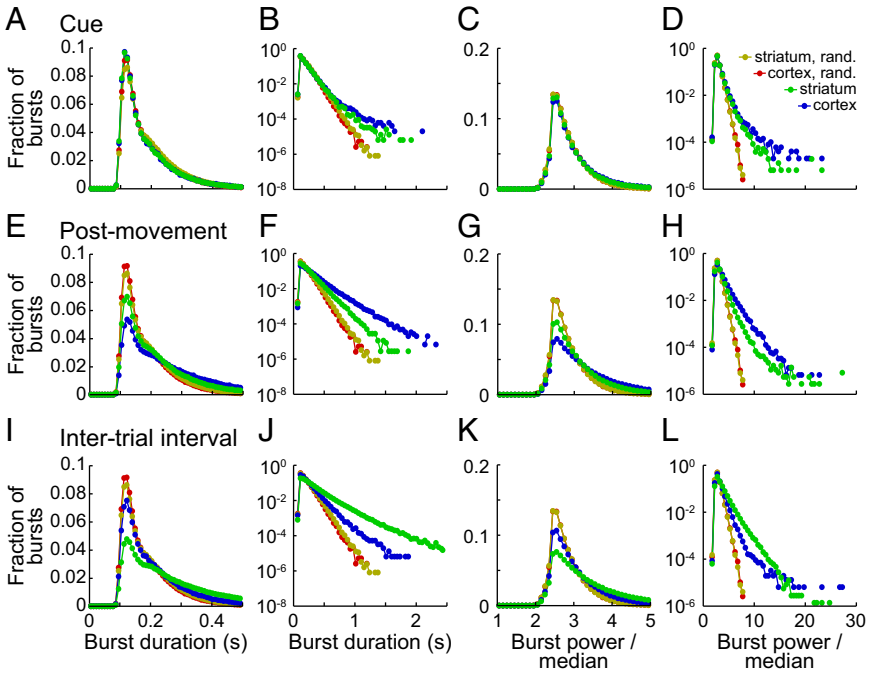

Fig. 6. Histograms showing the distributions of duration and power of bursts with peaks detected during the cue period (*A–D*), postmovement period (*E–H*), and ITI (*I–L*). Data were aggregated across both tasks and both monkeys for the motor cortex (blue) and striatum (green). Plots are paired, with the peaks of the distributions on a fine scale on the left and the logarithms of the distributions on a coarse scale on the right. The first two columns show durations, and the last two show power averaged over the whole burst. Results aggregated across all task periods are also shown for the phase-randomized counterparts of the signals from motor cortex (red) and striatum (gold).

many regions of the central nervous system, a substantial fraction of the beta bursts that follow task completion could be related to modifying (in error trials) or to maintaining (in correct trials) the strengths of the connections involved in task performance. The details of timing and selectivity for error or correct performance could vary from region to region.

Potential Implications for Beta Activity in Parkinson's Disease. Beta-band oscillations are best known as antimovement neural signals, exaggerated in patients with Parkinson's disease, and are the targets of therapeutic interventions to minimize their power. We note several features of this pathological beta rhythm compared with characteristics of healthy beta rhythm that we describe here. First, we found that on a trial-by-trial basis, the timing of bursts of beta power was highly variable in normal subjects repetitively performing a given task. In comparison, in Parkinson's patients off medication, Little et al. (34) reported that patients with the most severe motor symptoms had extremely low variation in power in the beta band, in some cases as low as those for our randomized signals. Second, we found that beta bursts were mainly brief, but Parkinson's patients off medication have been shown to exhibit an abnormally large proportion of "long" episodes (>100 ms) of beta-band phase-locking at phases that promote higher beta power (21). Abnormal prolongation of beta oscillation could be due in part to an abnormal thalamocortico-basal ganglia network resonance of the kind found by Moran et al. (35) in 6-hydroxydopamine model parkinsonian rats. In contrast, the durations of the beta bursts that we describe accord with the durations of beta oscillations evoked in healthy human subjects by the experimental delivery of a single transcranial magnetic stimulation pulse to parietal cortex, circa one or two cycles of oscillation occurring over widespread cortical regions (36).

Based on these findings, we suggest that the brevity of beta bursts could be critical to normal beta-band function, and that

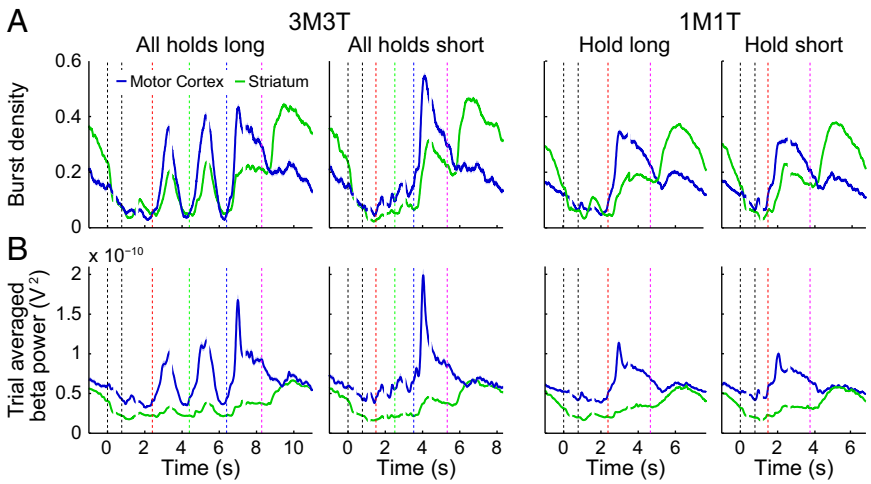

Fig. 7. Burst density (*A*) and beta-band power (13–30 Hz; *B*) averaged over trials for two timing patterns in each task. Breaks in traces mark the boundaries between panels that were aligned to different task events. Event markers are colored as in Fig. 1. Shading shows ±2 SEM.

the pathological prolongation of beta bursts could, in particular, be critical to the parkinsonian state. If postperformance beta bursts represent brief messages regarding the retrospective evaluation of task performance, and potentially affecting the next task performance, then a pathologically prolonged postperformance beta episode could lead to repetition of the same message many times, with a range of possible consequences. The exaggerated beta-band oscillations might simply crowd out the transmission of other messages. Because the durations of normal beta bursts, on the order of 50–150 ms, comport with time windows relevant to neuroplasticity and other features of neurotransmission, the bursts also could lead neural circuits to fall into fixed states, resulting in freezing or perseveration, states that are, like beta activity, decreased by dopamine replacement therapy (37). Thus, the indiscriminately high postperformance beta-band activity in Parkinson's patients could limit future choices for action by directly interfering with the normal adaptive mechanisms facilitated by postperformance beta bursts.

Materials and Methods

All methods were approved by the Committee on Animal Care at the Massachusetts Institute of Technology. Recordings were made in two female rhesus macaque monkeys (designated HH and JB) fitted with a titanium head post and a Delrin recording chamber in which electrodes were implanted for chronic recording, Recording sites were analyzed postmortem by histological analysis, as described in detail by Feingold et al. (38).

The monkeys, on a food- or water-restricted diet, were trained to manipulate a joystick with the right hand in a series of center-out-center movements, the details of which were specified in each trial by an array of visual cues. On correct completion of the instructed movements, the monkeys received liquefied food reward. Trials of a particular task type were grouped together in continuous blocks, with a short block of 1M1T at the beginning, followed by a long block of 3M3T, and then another short block of 1M1T. Monkeys were overtrained extensively on all variations of the task before recording began. We analyzed six sessions from monkey HH and seven sessions from monkey JB.

Further details are available in *SI Materials and Methods* and Table S2.

ACKNOWLEDGMENTS. We thank Drs. Naotaka Fujii, Theresa Desrochers, Robert Marini, Moshe Abeles, Christian Brown, Mark Histed, and Yasuo Kubota for their comments and advice, along with current and former laboratory members, including Dr. Naomi Hasegawa, Margo Cantor, Patricia Harlan, Christine Keller-McGandy, and Henry Hall, for their help with technical aspects of this study. This work was supported by the National Institutes of Health (Grant R01 NS025529), the Office of Naval Research (Grant N00014-07-1-0903), and the Defense Advanced Research Projects Agency (Grant NBCHC070105).

1. Neuper C, Wortz M, Pfurtscheller G (2006) ERD/ERS patterns reflecting sensorimotor activation and deactivation. *Prog Brain Res* 159:211–222.
2. Stancak A, Jr, Pfurtscheller G (1996) Event-related desynchronisation of central beta-rhythms during brisk and slow self-paced finger movements of dominant and non-dominant hand. *Brain Res Cogn Brain Res* 4(3):171–183.
3. Sanes JN, Donoghue JP (1993) Oscillations in local field potentials of the primate motor cortex during voluntary movement. *Proc Natl Acad Sci USA* 90(10):4470–4474.
4. Rubino D, Robbins KA, Hatsopoulos NG (2006) Propagating waves mediate information transfer in the motor cortex. *Nat Neurosci* 9(12):1549–1557.
5. Reimer J, Hatsopoulos NG (2010) Periodicity and evoked responses in motor cortex. *J Neurosci* 30(34):11506–11515.
6. Brown P, et al. (2001) Dopamine dependency of oscillations between subthalamic nucleus and pallidum in Parkinson's disease. *J Neurosci* 21(3):1033–1038.
7. Cassidy M, et al. (2002) Movement-related changes in synchronization in the human basal ganglia. *Brain* 125(Pt 6):1235–1246.
8. Marsden JF, Limousin-Dowsey P, Ashby P, Pollak P, Brown P (2001) Subthalamic nucleus, sensorimotor cortex and muscle interrelationships in Parkinson's disease. *Brain* 124(Pt 2):378–388.
9. Oswal A, Brown P, Litvak V (2013) Synchronized neural oscillations and the pathophysiology of Parkinson's disease. *Curr Opin Neurol* 26(6):662–670.
10. Williams D, et al. (2002) Dopamine-dependent changes in the functional connectivity between basal ganglia and cerebral cortex in humans. *Brain* 125(Pt 7):1558–1569.
11. Hammond C, Bergman H, Brown P (2007) Pathological synchronization in Parkinson's disease: networks, models and treatments. *Trends Neurosci* 30(7):357–364.
12. Murthy VN, Fetz EE (1992) Coherent 25- to 35-Hz oscillations in the sensorimotor cortex of awake behaving monkeys. *Proc Natl Acad Sci USA* 89(12):5670–5674.
13. Murthy VN, Fetz EE (1996) Oscillatory activity in sensorimotor cortex of awake monkeys: Synchronization of local field potentials and relation to behavior. *J Neurophysiol* 76(6):3949–3967.
14. Pfurtscheller G, Stancak A, Jr, Neuper C (1996) Post-movement beta synchronization: A correlate of an idling motor area? *Electroencephalogr Clin Neurophysiol* 98(4): 281–293.
15. Leventhal DK, et al. (2012) Basal ganglia beta oscillations accompany cue utilization. *Neuron* 73(3):523–536.
16. Barnes T, Kubota Y, Hu D, Jin DZ, Graybiel AM (2005) Activity of striatal neurons reflects dynamic encoding and recoding of procedural memories. *Nature* 437(7062): 1158–1161.
17. Fujii N, Graybiel A (2003) Representation of action sequence boundaries by macaque prefrontal cortical neurons. *Science* 301(5637):1246–1249.
18. Thorn CA, Atallah H, Howe M, Graybiel A (2010) Differential dynamics of activity changes in dorsolateral and dorsomedial striatal loops during learning. *Neuron* 66(5): 781–795.
19. Smith KS, Graybiel AM (2013) A dual operator view of habitual behavior reflecting cortical and striatal dynamics. *Neuron* 79(2):361–374.
20. Jin X, Costa RM (2010) Start/stop signals emerge in nigrostriatal circuits during sequence learning. *Nature* 466(7305):457–462.
21. Cagnan H, Duff EP, Brown P (2015) The relative phases of basal ganglia activities dynamically shape effective connectivity in Parkinson's disease. *Brain* 138(Pt 6): 1667–1678.
22. von Nicolai C, et al. (2014) Corticostriatal coordination through coherent phase-amplitude coupling. *J Neurosci* 34(17):5938–5948.
23. Fujisawa S, Buzsaki G (2011) A 4-Hz oscillation adaptively synchronizes prefrontal, VTA, and hippocampal activities. *Neuron* 72(1):153–165.
24. Tort ABL, et al. (2008) Dynamic cross-frequency couplings of local field potential oscillations in rat striatum and hippocampus during performance of a T-maze task. *Proc Natl Acad Sci USA* 105(51):20517–20522.
25. Masimore B, Schmitzer-Torbert NC, Kakalios J, Redish AD (2005) Transient striatal gamma local field potentials signal movement initiation in rats. *Neuroreport* 16(18): 2021–2024.
26. Howe MW, Atallah HE, McCool A, Gibson DJ, Graybiel AM (2011) Habit learning is associated with major shifts in frequencies of oscillatory activity and synchronized spike firing in striatum. *Proc Natl Acad Sci USA* 108(40):16801–16806.
27. Antzoulatos EG, Miller EK (2014) Increases in functional connectivity between prefrontal cortex and striatum during category learning. *Neuron* 83(1):216–225.
28. Buschman TJ, Denovellis EL, Diogo C, Bullock D, Miller EK (2012) Synchronous oscillatory neural ensembles for rules in the prefrontal cortex. *Neuron* 76(4):838–846.
29. Saalmann YB, Pinsk MA, Wang L, Li X, Kastner S (2012) The pulvinar regulates information transmission between cortical areas based on attention demands. *Science* 337(6095):753–756.
30. Tan H, Jenkinson N, Brown P (2014) Dynamic neural correlates of motor error monitoring and adaptation during trial-to-trial learning. *J Neurosci* 34(16):5678–5688.
31. Tan H, et al. (2014) Human subthalamic nucleus in movement error detection and its evaluation during visuomotor adaptation. *J Neurosci* 34(50):16744–16754.
32. Desrochers TM, Amemori K, Graybiel AM (2015) Habit learning by naive macaques is marked by response sharpening of striatal neurons representing the cost and outcome of acquired action sequences. *Neuron* 87(4):853–68.
33. Engel AK, Fries P (2010) Beta-band oscillations: signalling the status quo? *Curr Opin Neurobiol* 20(2):156–165.
34. Little S, Pogosyan A, Kuhn AA, Brown P (2012) Beta band stability over time correlates with parkinsonian rigidity and bradykinesia. *Exp Neurol* 236(2):383–388.
35. Moran RJ, et al. (2011) Alterations in brain connectivity underlying beta oscillations in parkinsonism. *PLoS Comput Biol* 7(8):e1002124.
36. Johnson JS, Kundu B, Casali AG, Postle BR (2012) Task-dependent changes in cortical excitability and effective connectivity: A combined TMS-EEG study. *J Neurophysiol* 107(9):2383–2392.
37. Rutledge RB, et al. (2009) Dopaminergic drugs modulate learning rates and perseveration in Parkinson's patients in a dynamic foraging task. *J Neurosci* 29(48):15104–15114.
38. Feingold J, et al. (2012) A system for recording neural activity chronically and simultaneously from multiple cortical and subcortical regions in nonhuman primates. *J Neurophysiol* 107(7):1979–1995.
39. Paxinos G, Huang X-F, Toga AW (1999) *The Rhesus Monkey Brain in Stereotaxic Coordinates* (Academic Press, San Diego).
40. Künzle H (1975) Bilateral projections from precentral motor cortex to the putamen and other parts of the basal ganglia: An autoradiographic study in *Macaca fascicularis*. *Brain Res* 88(2):195–209.
41. Courtemanche R, Fujii N, Graybiel A (2003) Synchronous, focally modulated β-band oscillations characterize local field potential activity in the striatum of awake behaving monkeys. *J Neurosci* 23(37):11741–11752.